Spatially Resolved X-Ray Spectroscopy of Kepler's Supernova Remnant: Distinct Properties of the Circumstellar Medium and the Ejecta

Lei Sun (孫磊) and Yang Chen (陳陽)

Department of Astronomy, Nanjing University, Nanjing 210023, People's Republic of China

Abstract: Kepler's supernova remnant (SNR) is believed to result from a Type Ia supernova, but be interacting with dense circumstellar material (CSM), which makes its progenitor system a mystery. Using the deep Chandra data and an adaptive binning algorithm, we analyse the spectra from tessellated regions in Kepler's SNR. For the first time, we map out the detailed spatial distributions of multiple physical parameters. We distinguish the CSM from the ejecta based on the $[O]/[Fe]_L$ and $[Mg]/[Fe]_L$ abundance ratios. The total hydrogen mass of the shocked CSM was estimated to be $\sim 1.4 M_\odot$ and the mean [Mg]/[O] to be ~ 1.14, which can be reproduced by an asymptotic giant branch donor star with initial mass of $\sim 4 M_\odot$. The abundance ratios from the shocked ejecta are well compatible with the predicted results from spherical delayed-detonation models for Type Ia supernovae. We also find that the two "ears" are dominated by Si- and S-rich ejecta, thus favoring a pre-explosion jets scenario.

Observations & Spectral Fitting Results

Kepler's SNR is one of the mostly studied historical SNRs. The deep Chandra observations with a total effective exposure of ~741 ks provides us an excellent opportunity to carry out elaborate spatially-resolved spectroscopy analysis.

Using the Weighted Voronoi Tessellation (WVT) adaptive binning algorithm (Cappellari & Copin 2003, Diehl & Statler 2006), we divided the whole remnant into 4671 tessellated regions, and each region contains ~6400 counts (S/N~80). We extracted X-ray spectra in 0.3-8.0 keV band and performed unified spectral fitting for each of the regions. The spectrum model contained two major components: a thermal emission component from non-equilibrium ionization (NEI) plasma, and a non-thermal emission component from shock accelerated electrons. Based on the spectral fitting results, we constructed the spatial distribution maps of multiple physical parameters over the remnant (Figure 2).

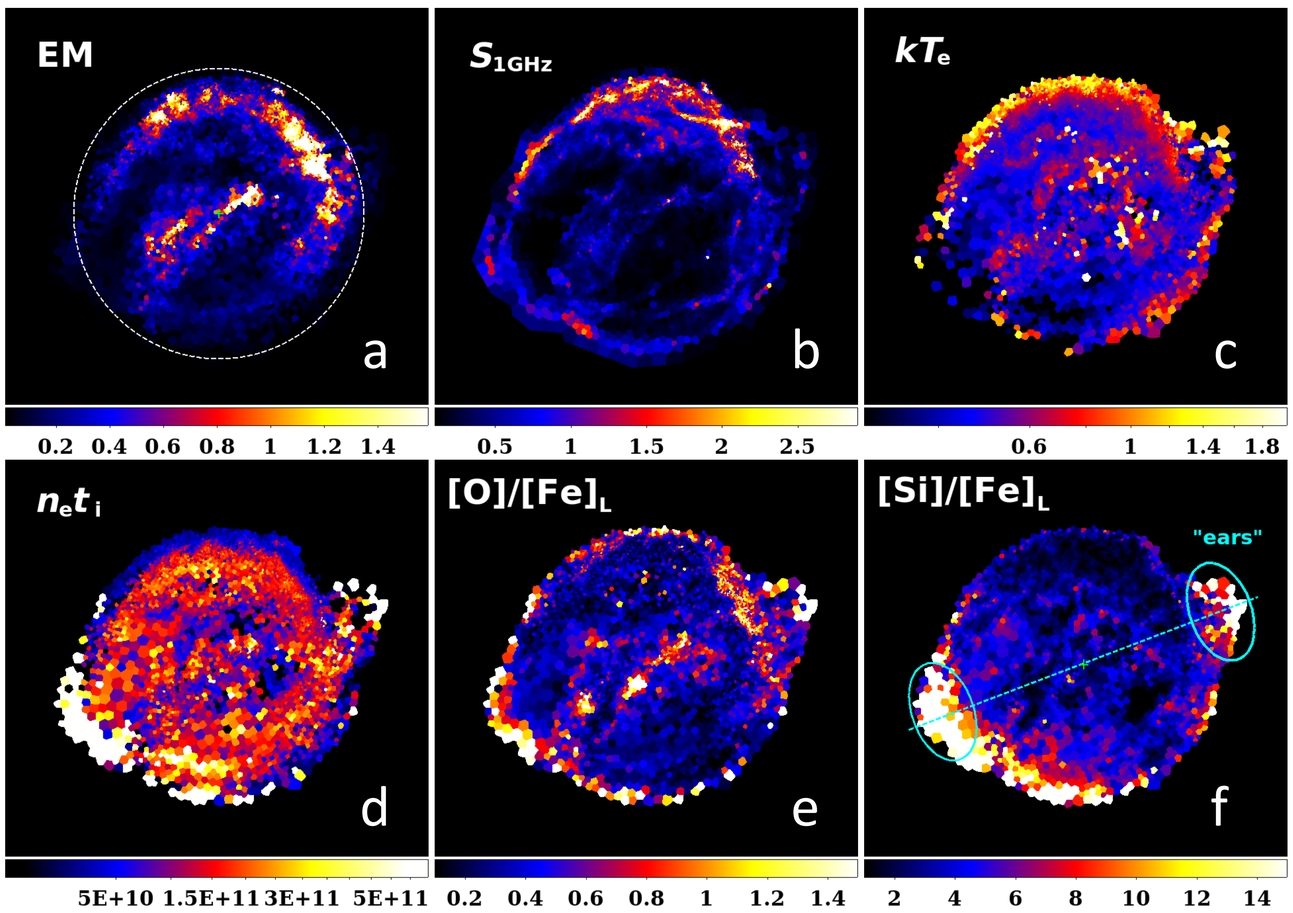

Figure 2. Maps of: (a) specific EM (10^{-5} cm^{-5}arcsec^{-2}), (b) brightness of radio emission at 1GHz (mJy arcsec^{-2}), (c) electron temperature (keV), (d) ionization parameter (cm^{-3}s), (e) $[O]/[Fe]_L$ abundance ratio, and (f) $[Si]/[Fe]_L$ abundance ratio.

Implications for Progenitor and Explosion Mechanism

We estimated the total hydrogen mass of the shocked CSM to be $\sim 1.4 M_\odot$ and the [Mg]/[O] to be ~ 1.14, which can be reproduced by an AGB donor with initial mass of $\sim 4 M_\odot$ (Karakas 2010). The abundance ratios of the ejecta are well compatible with the predicted results from DDT models for SN Ia (Seitenzahl et al. 2013). Additionally, the ejecta-dominated "ears" structure favors a pre-explosion jets scenario (Tsebrenko & Soker 2013).

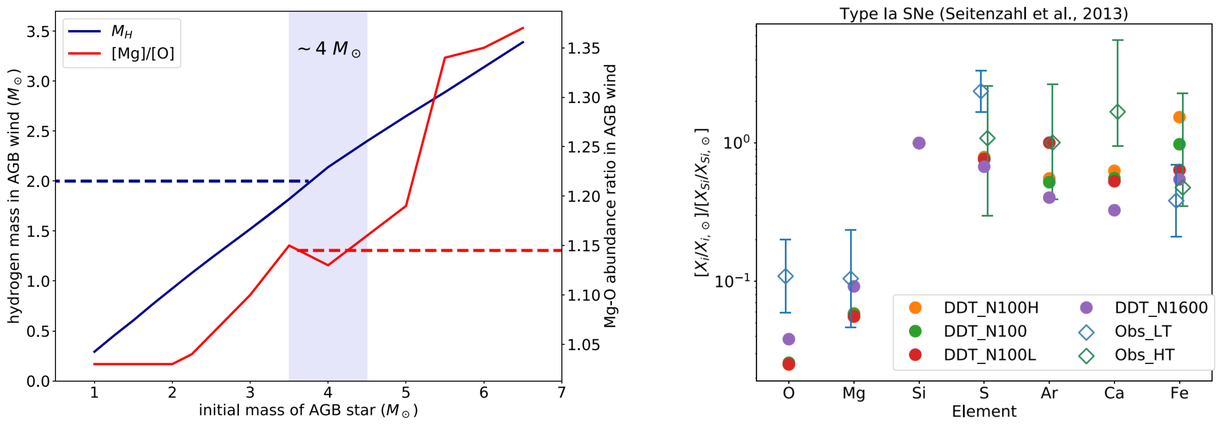

Figure 4. *Left*: hydrogen mass and [Mg]/[O] in AGB wind, based on the results of Karakas (2010). *Right*: metal abundance ratios of the ejecta in Kepler, compared with the predicted results of 3D DDT models with multi-spot ignition, from Seitenzahl et al. (2013).

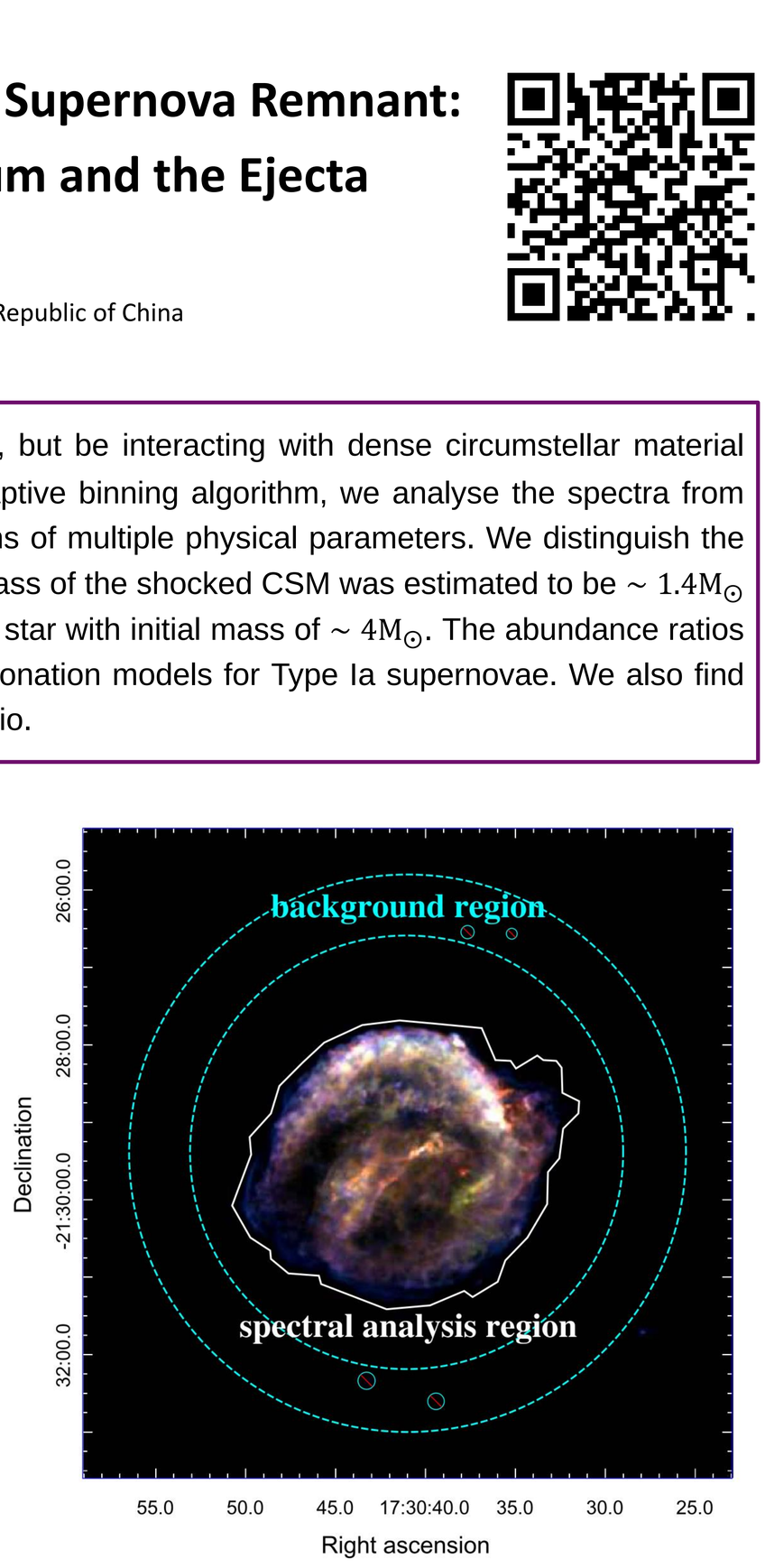

Figure 1. Merged image of the Chandra ACIS-S observations with an effective exposure time of 741 ks. Red: 0.3–0.72 keV; green: 0.72–1.7 keV; blue: 1.7–8.0 keV.

Distinguish the CSM from SN Ejecta

It can be found that high $[O]/[Fe]_L$ and $[Mg]/[Fe]_L$ ratios mainly appear in NW, central bar-like region, and outer regions of the remnant, indicating they are dominated by CSM. The two "ears" are dominated by SN ejecta, characterized by high $[Si]/[Fe]_L$.

We further distinguished the CSM based on the probability distribution functions (PDFs) of $[O]/[Fe]_L$ and $[Mg]/[Fe]_L$, which can be fitted by double-Gaussian models (Figure 3 & Table 1).

Table 1. Double-Gaussian Fitting Results of the PDFs

	CSM		Ejecta	
	$[O]/[Fe]_L$	$[Mg]/[Fe]_L$	$[O]/[Fe]_L$	$[Mg]/[Fe]_L$
Peak Ratio	$0.77^{+0.30}_{-0.23}$	$1.11^{+0.46}_{-0.32}$	$0.31^{+0.17}_{-0.10}$	$0.38^{+0.36}_{-0.19}$
Total $n_e M_{gas}$ ($M_\odot$ cm^{-3})[a]	~15	~6	~22	~31

[a] Assuminig a distance to Kepler of 5.1 kpc.

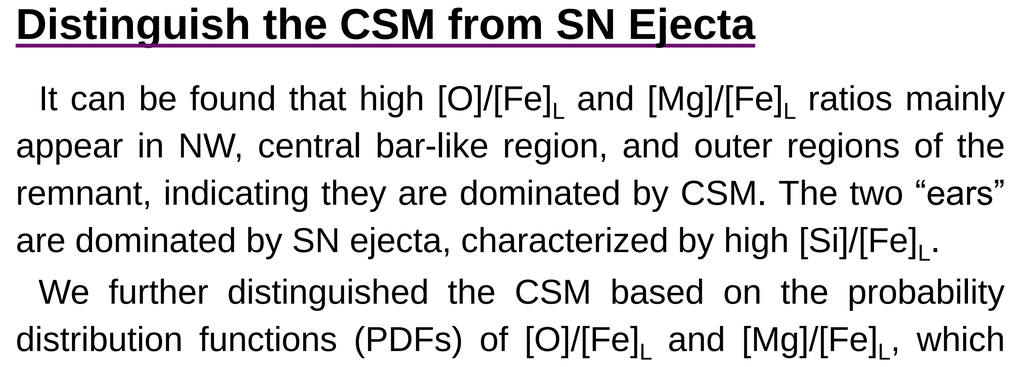

Figure 3. The PDFs and double-Gaussian fitting of $[O]/[Fe]_L$ and $[Mg]/[Fe]_L$.

Reference:

Cappellari, M., & Copin, Y. 2003, MNRAS, 342, 345
Diehl, S., & Statler, T. S. 2006, MNRAS, 368, 497
Karakas, A. I. 2010, MNRAS, 403, 1413
Seitenzahl, I. R., Ciaraldi-Schoolmann, F., Röpke, F. K., et al. 2013, MNRAS, 429, 1156
Tsebrenko, D., & Soker, N. 2013, MNRAS, 435, 320

Contact:

lsun_94@foxmail.com **or** ygchen@nju.edu.cn